IJIRSET
International Journal of Innovative Research in
SCIENCE | ENGINEERING | TECHNOLOGY

e-ISSN: 2319-8753 | p-ISSN: 2347-6710

INTERNATIONAL JOURNAL OF INNOVATIVE RESEARCH

IN SCIENCE | ENGINEERING | TECHNOLOGY

Volume 13, Issue 4, April 2024

ISSN INTERNATIONAL STANDARD SERIAL NUMBER INDIA

Impact Factor: 8.423

9940 572 462 | 6381 907 438 | ijirset@gmail.com | www.ijirset.com

International Journal of Innovative Research in Science, Engineering and Technology (IJIRSET)

| e-ISSN: 2319-8753, p-ISSN: 2347-6710| www.ijirset.com | Impact Factor: 8.423| A Monthly Peer Reviewed & Referred Journal |

|| Volume 13, Issue 4, April 2024 ||

| DOI:10.15680/IJIRSET.2024.1304086 |

Microscopic investigation on growth of large grain $Si_{1-x}Ge_x$ thin film at low temperatures

T. Sain, J. Kavitha

Department of Physics, Sathyabama Institute of Science and Technology, Chennai, Tamil Nadu, India

ABSTRACT: A systematic approach towards realizing Si1-xGex alloy in its large-grained polycrystalline form and at a temperature nearing flexible electronics application has been made in this work. Polycrystalline (poly)- Si1-xGex alloy thin film was realized at a temperature (< 350 °C), i.e. much lower than its bulk crystallization temperature using catalytic Al-induced crystallization (AIC) of amorphous (a)-Ge/ AlOx /Al on Si (100) substrate. Our results show that the onset of crystallization was preceded by the alloying between Si and Ge in the presence of Al to form a-SiGe phase. The alloying that leads to the formation of poly- Si1-xGex alloy was confined to microscopic regions wherein Al induces a layer exchange of the original a-Ge/Al bilayer during the AIC process. Further, using the method of AIC and with a modified layer structure of a-Si0.2Ge0.8(100nm)/AlOx(~1nm)/c-Al(50 nm), poly- Si1-xGex alloy thin film with large grain size ~ 50 µm was achieved on cost-effective glass substrates at temperature as low as 350 ℃ with full surface coverage.

The grain growth of poly- Si1-xGex is probed using microscopic techniques. Moreover, the interesting phenomenon of layer exchange associated with this process which finally results in the realization of poly- Si1-xGex on low-cost substrates is visualized through energy-dispersive X-ray spectroscopy and optical microscopy. Thus, the achievement of large grain as well as low crystallization temperature directs the way for poly- Si1-xGex to be a promising material for low temperature- budget applications.

KEYWORDS: SiGe thin film, low temperature crystallization, Al induced crystallization, large grain

I. INTRODUCTION

The group IV alloy semiconductor (SC) SiGe have a stoichiometry dependent wide range of tunable properties. As such, large grain polycrystalline (poly)-SiGe thin film has several potential applications in high efficiency solar cells, thin-film transistors, flexible electronics, photodiode, active matrix-LCD, IR image sensors and integrated electronics [1–4]. In comparison to other crystallization techniques like solid phase crystallization (SPC) and laser annealing (LA), poly-SC thin films achieved using metal induced crystallization (MIC) tend to have relatively larger grain size [5–7]. Hence, MIC has been extensively used for catalytic crystallization of amorphous(a) Si, Ge, and their alloy (SiGe) thin films at low temperatures [8–12]. The formation temperature of poly-SiGe thin film phase achieved with MIC is generally much lower than the temperatures reported using SPC and LA [13,14]. It is reported that poly-SiGe thin film can be obtained at temperatures below 450 ºC using Al induced crystallization (AIC) [5,15,16]. It may also be noted that Al forms a eutectic with Ge and Si at 420 and 577 ºC, respectively [17,18]. On several occasions, the AIC process also causes an inversion of the original Al/SC bilayer structure and it is known as Al induced layer exchange (ALILE) process [19]. ALILE depends on many parameters like the interface oxide (and its thickness), microstructure (and thickness) of crystalline (c)-Al film, the thickness ratio of Al:SC bilayer, and annealing temperatures [20–22]. The poly-SiGe obtained below the above-mentioned eutectic temperatures using AIC process enables the etching-off of the metallic Al and hence makes these films suitable for low thermal budget applications [12]. However, plastic and polymer substrates that are explored for very low thermal budget applications still require lower crystallization temperatures i.e. < 300 °C. Hence, the realization of poly-SiGe using AIC accompanied by layer exchange or ALILE at a temperature lower than the eutectic temperature of the metal-SC system is of utmost importance.

In this paper, we report the realization of poly-SiGe thin film on Si (100) below 300 °C by employing AIC in a-Ge/c-Al bilayer on Si (100). The importance of layer exchange in the initiation of SiGe alloying process and subsequent formation of poly-SiGe in this system is discussed. Further, towards improving the crystal quality with large grain size, the realization of poly-SiGe thin film on cost cost-friendly glass substrate using AIC in a-SiGe/c-Al bilayer is demonstrated.

| e-ISSN: 2319-8753, p-ISSN: 2347-6710| www.ijirset.com | Impact Factor: 8.423| A Monthly Peer Reviewed & Referred Journal |

|| Volume 13, Issue 4, April 2024 ||

| DOI:10.15680/IJIRSET.2024.1304086 |

II. METHODOLOGY

In the present study, Al thin film (~ 50 nm) was evaporated onto cleaned Si (100) wafer substrates using electron beam evaporation system. Diffusion controlling surface native oxide layer (AlOx) was formed on top of the Al thin film by exposing it to ambient for ~ 1 hour. Thereafter, ~ 100 nm thick a-Ge thin film was deposited onto AlOx/c-Al/Si(100) thin film by electron beam evaporation. These samples were then isothermally vacuum (~10-8 mbar) annealed at 280 ºC for 5 and 10 hrs. For brevity S1, S2 and S3 will be used to refer to the pristine sample, sample annealed for 5 hrs, and sample annealed for 10 hrs, respectively. A second set of samples with layer structure a-Si0.2Ge0.8(100nm)/AlOx(~1nm)/c-Al(50 nm) was deposited on corning glass substrate. a-Si0.2Ge0.8(100nm) and c-Al(50 nm) was deposited using electron beam evaporation system. Isothermal annealing at 350 ℃ was carried out on the second sample set in N2 flow ambience. A schematic of the sample layer structure along with the mechanism of AIC is illustrated in Figure 1. The microstructural features of the samples along with their evolution in elemental composition upon annealing were studied using Field Emission Scanning Electron Microscopic (FESEM) and Energy-Dispersive X-Ray Spectroscopic (EDS) studies in a Carl Ziess FESEM (Supra 55). The structural and phase characteristics of all the samples were investigated using Grazing Incidence X-Ray Diffraction (GIXRD) and Raman spectroscopy. The GIXRD measurements were performed in STOE (Germany) diffractometer using Cu kα (λ = 1.5406 Å) in the parallel beam geometry. The Raman spectral measurements were performed in a Raman microscope (inVia, Renishaw, UK) using green light laser 514.5 nm as the excitation source along with 1800 gr/mm grating and CCD detector in the backscattering configuration. The optical images were acquired using a Axio Vert.A1 (Carl Zeiss) optical microscope.

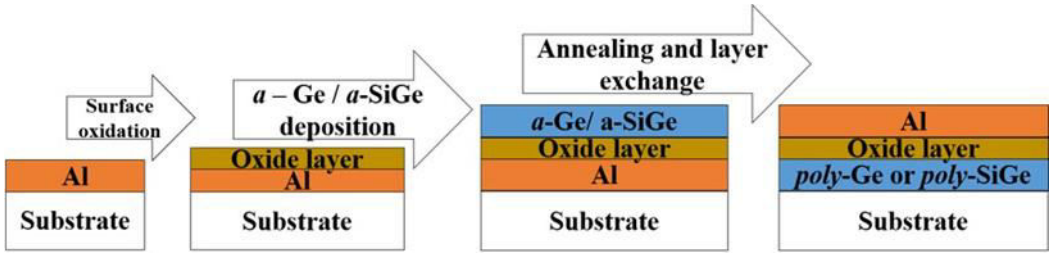

Figure 1. (Colour online) Schematic of the sample layer structure and the mechanism of layer inversion in Al induced crystallization process.

III. EXPERIMENTAL RESULTS

The effect of annealing on the layer structure and microstructural features of the sample were investigated using FESEM. The FESEM micrographs of the S1, S2 and S3 samples are shown in Figure 2. The surface micrograph of the S1 sample shown in Figure 2(a) consists of fine granular agglomerates pertaining to *a*-Ge thin film. The distinct layer structure of *a*-Ge/*c*-Al on Si(100) in the S1 sample is illustrated by the cross-sectional SEM micrograph shown as an inset in Figure 2(a). Subsequently, upon vacuum annealing the sample at 280 ºC for 5 hrs, the distinct layer structure disappears as evident from the inset in Figure 2(b). Additionally, two distinct region-of-interests (RoIs) with different microstructural features could be observed in surface micrograph of the S2 sample (see Figure 2(b)). These RoIs are characterized by circle like discrete bright patterns (RoI-1) visible on region with relatively darker background (RoI-2). Further evolution in the microstructural features ensue upon increasing the annealing duration from 5 to 10 hrs in the S3 sample as seen in the SEM micrograph (Figure 2(c)). The circle like pattern observed in S2 sample (RoI-1) has grown in size and coalesce leading to the overall increase in the volume fraction of the RoI-1 in the S3 sample. This is accompanied by the shrinkage in the volume fraction of RoI-2. The layer structure and elemental composition of these two microscopic RoIs were further investigated using EDS.

The EDS spectrum for all the samples is shown in Figure 3. The spectrum for S1 sample exhibit peaks arising from the top Ge thin film layer and the underlying Al layers at ~ 1.2 and 1.5 keV, respectively. Any subsequent changes in the layer structure of the bilayer upon annealing will manifest as a change in the relative intensities of the Ge and Al peaks. This is because the intensity of the X-rays emanating from the underlying layer will be attenuated through the mass absorption co-efficient of the top layer. The EDS spectrum from RoI-2 of sample S2 is largely similar to the EDS spectrum of sample S1, except for a slight decrease in Ge peak intensity. However, the relative intensity of the Ge and Al peaks in the EDS spectra from RoI-1 of sample S2 shows significant changes (Figure 3). The Al peak intensity in

| e-ISSN: 2319-8753, p-ISSN: 2347-6710| www.ijirset.com | Impact Factor: 8.423| A Monthly Peer Reviewed & Referred Journal |

|| Volume 13, Issue 4, April 2024 ||

| DOI:10.15680/IJIRSET.2024.1304086 |

RoI-1 of sample S2 has increased with a corresponding decrease in the Ge peak intensity. The increase in Al peak intensity is attributed to the migration of Al from the underlying Al layer to the film's surface. This migration is induced by stress relaxation in the Al layer which is strained by the in-diffusion of Ge. Similar, migrational mechanism were also observed in *a*-Si/Au bilayer system, wherein the strain generated by the in-diffusion of Si in the Au layer is relief by migration of metallic Au to the top surface [8,19]. Further, changes in the EDS spectra of these two RoIs upon increasing the annealing time duration to 10 hrs (S3 sample) is also shown in Figure 3. The EDS spectrum from RoI-2 of sample S3 is not very different from the spectra of S1 or RoI-2 of S2 samples. The diffusion of Ge into Al layer in RoI-2 is still not significant enough to cause a reverse migration of the Al layer. Whereas in the RoI-1of S3, continued diffusion of Ge into Al layer and migration of Al to the film's surface has led to a layer inversion in these regions. This is evident from the EDS spectra of RoI-1 of S3 where Al peak intensity has drastically increased and Ge peak intensity diminished. Further details about the structural and phase characteristics of the samples were investigated with GIXRD and Raman spectroscopy.

The GIXRD pattern of the as-deposited and annealed samples are shown in Figure 4. The intense peak at 2θ ~ 56.1° arises from the underlying Si substrate. The pattern of the S1 sample shows that the as-deposited Ge thin film is amorphous in nature. For the S2 sample, four peaks could be clearly indexed. The peaks at 2θ ~ 27.3°, 45.4° and 53.9° correspond to diffractions from Ge (111), Ge (220) and Ge (311) planes of *poly*-Ge phase. The peak at 2θ ~ 38.7° belongs to Al (111) from the underlying crystalline Al film. It is seen that annealing of S1 sample at 280 °C for 5 hrs leads to AIC of *a*-Ge into poly-Ge phase. The crystallization temperature T_c of Ge itself is very low compared to its bulk T_c ~ 500°C [23]. Additionally, the observed Ge peaks for S2 sample are asymmetric due to the presence of small noticeable shoulders on the higher 2θ side (see Figure 4). With further increase in annealing duration to 10 hrs in S3 sample, the asymmetry in the Ge peaks of S2 disappears

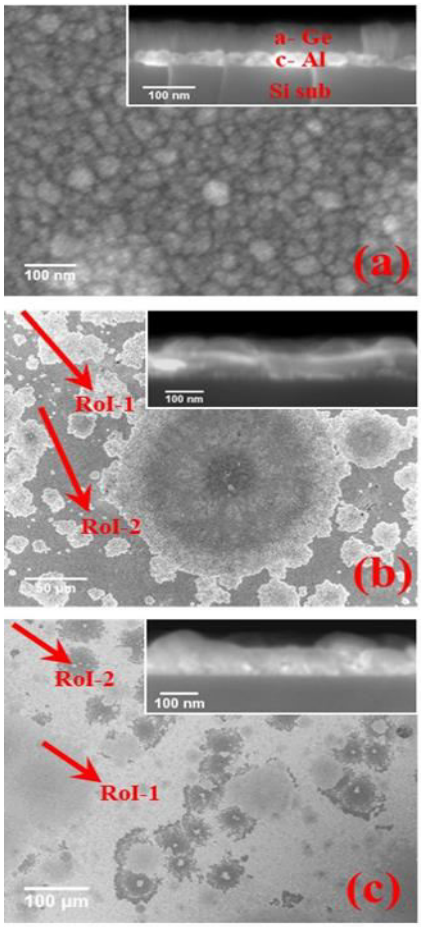

Figure 2. (Color online) FESEM micrographs showing (a) surface of S1; (b) surface of S2 and (c) surface of S3. The corresponding insets in each figure are the cross section of each sample.

| e-ISSN: 2319-8753, p-ISSN: 2347-6710| www.ijirset.com | Impact Factor: 8.423| A Monthly Peer Reviewed & Referred Journal |

|| Volume 13, Issue 4, April 2024 ||

| DOI:10.15680/IJIRSET.2024.1304086 |

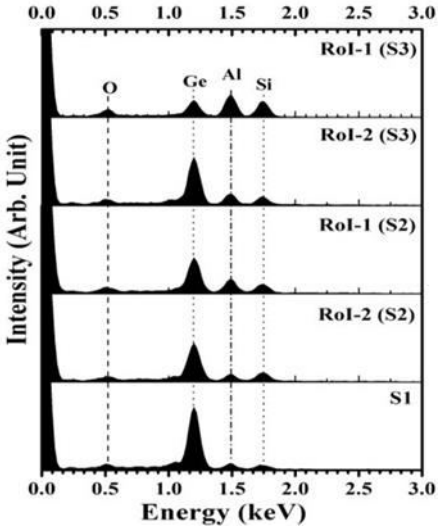

Figure 3. EDS spectra from different microscopic region-of-interests (RoIs) of S1, S2 and S3 sample.

and peaks corresponding to *poly*-SiGe alloy phase appears in the XRD pattern of S3. In addition to the peaks observed in S2 that belongs to *poly*-Ge and *c*-Al phases, two additional peaks could be indexed at 2θ ~ 28.1° and 46.1° in the XRD pattern of S3 sample. These peaks correspond to SiGe (111) and SiGe (220) diffraction planes, respectively. It shows that in the S3 sample, along with AIC of *a*-Ge, alloying of the diffused Ge with Si occurs leading to the formation of *poly*-SiGe phase. To gain more detailed insights into the phases present in different RoIs of S2 and S3 samples, micro-Raman studies were performed.

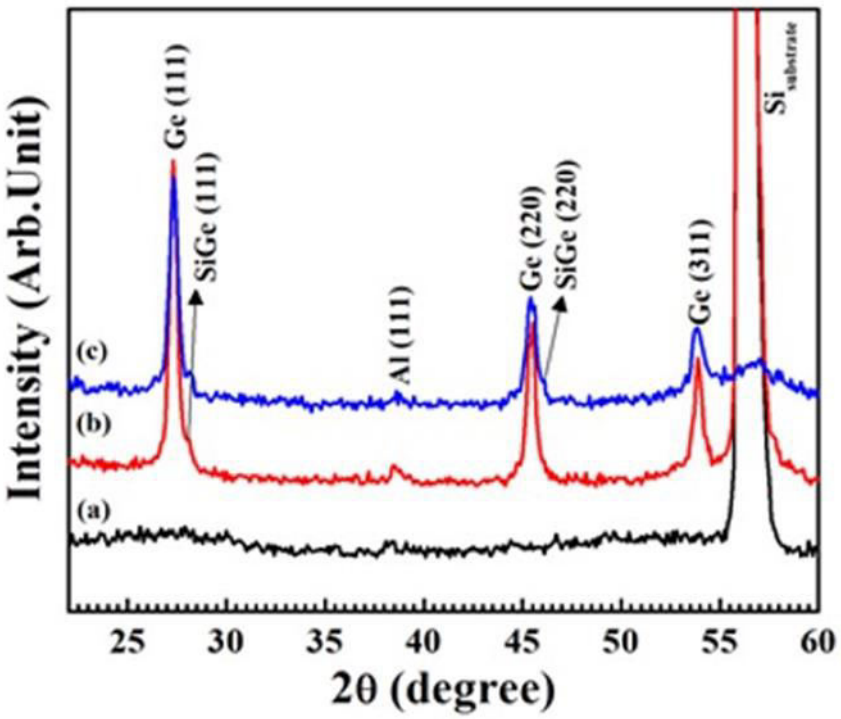

Figure 4. (Color online) GIXRD pattern of (a) as deposited sample S1, (b) 5 hrs annealed sample S2 and (c) 10 hrs annealed sample S3.

| e-ISSN: 2319-8753, p-ISSN: 2347-6710| www.ijirset.com | Impact Factor: 8.423| A Monthly Peer Reviewed & Referred Journal |

|| Volume 13, Issue 4, April 2024 ||

| DOI:10.15680/IJIRSET.2024.1304086 |

The Raman spectra for the pristine and the isothermally annealed samples are shown in Figure 5. The Raman spectrum of the S1 sample exhibits only a peak at ~ 271.6 cm^{-1} corresponding to *a*-Ge [24]. The Raman spectrum acquired from RoI-1of S2 sample exhibit three main peaks at ~ 300, 383.8 and 521.2 cm^{-1}. While the peak at 521 cm^{-1} is attributed to Si substrate, the peak at 383.8 cm^{-1} corresponds to the vibration mode of Si—Ge bond in *a*-SiGe alloy phase [25–27]. The main peak at ~ 300 cm^{-1} consists of two peaks centered at ~ 292 and 298.5 cm^{-1}. Both these peaks belong to Ge—Ge modes. These Ge—Ge modes arise from the vibration of Ge in the neighborhood of Si in *a*-SiGe phase and the vibration of Ge in *poly*-Ge phase, respectively [27]. Whereas, in the RoI-2 of S2, the Ge—Ge mode at ~ 292 cm^{-1} is relatively much weaker and the Si—Ge mode from *a*-SiGe phase at ~ 384 cm^{-1} is almost negligible (see Figure 5). Further, Raman spectrum from the RoI-1 of S3 sample exhibit peaks at ~ 288.7 and 387 cm^{-1} apart from Si substrate peak as seen in Figure 5. The first peak corresponds to vibration mode of Ge—Ge bond in SiGe phase. It can be noted that the Ge—Ge mode due to *poly*-Ge that was visible at ~ 299 cm^{-1} in S2 (RoI-1) has almost disappeared after 10 hrs annealing in S3 sample. The second main peak at 387 cm^{-1} is a convolution of two peaks and can be resolves into two peaks at 384.3 and 390 cm^{-1}. This peak corresponds to Si—Ge modes in *a*-SiGe and *poly*-SiGe, respectively [27]. The Raman spectrum from RoI-2 of S3 sample on the other hand exhibits only a weak peak at ~ 289 cm^{-1}.

Now, it is clearly established from FESEM and EDS that the distinct layer structure of the S1 sample disappears in the annealed samples S2 and S3. While the microscopic regions identified as RoI-2 largely preserved the original architecture, substantial layer inversion could be observed only in RoI-1 of S2 and S3. It means that little Ge could diffuse towards the Si substrate in RoI-2 compared to RoI-1. Hence, AIC process in RoI-2 of S2 and S3 samples where layer exchange is not initiated are limited to crystallization of the *a*-Ge phase into *poly*-Ge phase as detected by both XRD and Raman. Without layer exchange, alloying is effectively not initiated. Whereas the AIC process in RoI-1 of S2 and S3 samples causes substantial inversion of the original Ge/Al bilayer layer due to the large amount of Ge in-diffusion into the Al layer. Hence, in RoI-1, formation of SiGe alloy phase could be observed in addition to crystallization of *a*-Ge into *poly*-Ge phase. The presence of both diffusing mobile Ge atoms and the Si─Si covalent bonds that are weakened in the vicinity of Al facilitates the initiation of alloying in RoI-1 during AIC [19]. Further, the extent of layer inversion process as well as the type of alloy phases formed during AIC depends on the annealing time duration. The layer inversion has just initiated upon isothermal annealing for 5 hrs in RoI-1of S2 (see EDS in Figure 3). Hence, the interface (I/F) near Si substrate i.e. Al-Si I/F is Ge limited and only *a*-SiGe phase could be observed in RoI-1 of S2 (see Raman in Figure 5). When annealing duration is increased to 10 hrs, the layer inversion in RoI-1 of S3 is almost complete along with a substantial increase in the volume fraction of RoI-1 (see SEM and EDS in Figure 2(c) and 3, respectively). Now, the I/F with Si substrate effectively become Ge-Si I/F due to the availability of Ge in excess of Al at the I/F with Si substrate. Consequently, AIC process in RoI-1 of S3 results in nucleation of *poly*-SiGe phase along with *a*-SiGe phase as detected by both XRD and Raman. It is thus found that poly-SiGe is realized at a low temperature of 280 °C which is much lower than its bulk crystallization temperature. This has become only possible as there is a balance between SiGe crystallization temperature and the change in interface energetics upon annealing the sample for 10 hrs.

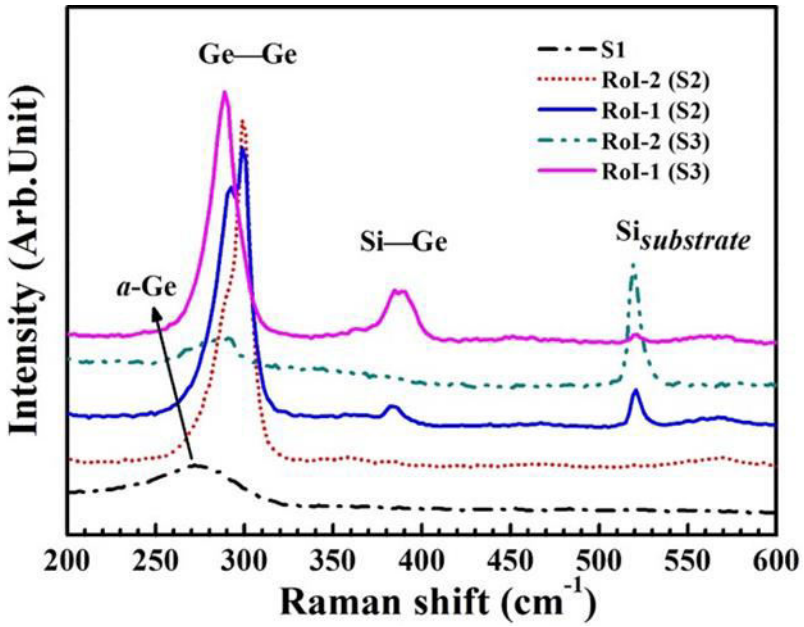

Figure 5. (Color online) Raman spectra from different microscopic RoIs of S1, S2 and S3 samples.

| e-ISSN: 2319-8753, p-ISSN: 2347-6710| www.ijirset.com | Impact Factor: 8.423| A Monthly Peer Reviewed & Referred Journal |

|| Volume 13, Issue 4, April 2024 ||

| DOI:10.15680/IJIRSET.2024.1304086 |

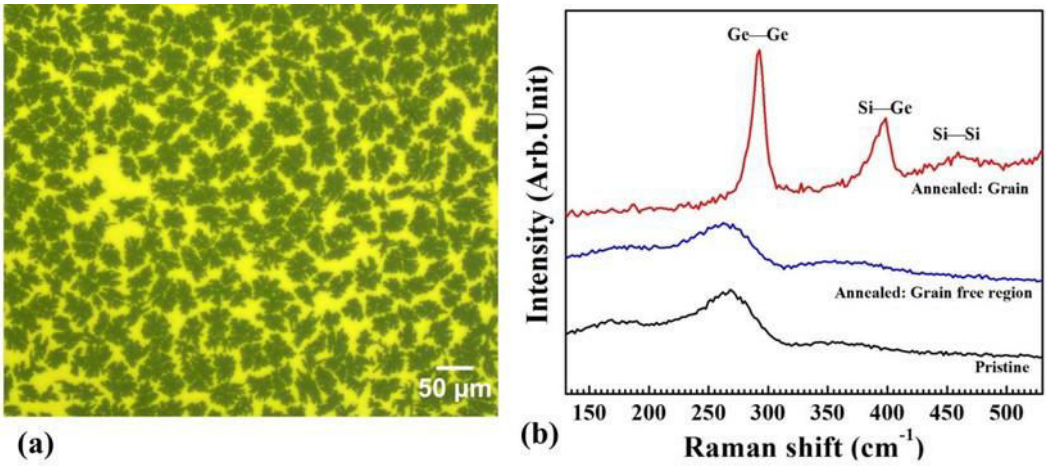

Figure 6. (Color online) (a) Optical micrograph of the annealed sample deposited CG substrate acquired from backside and (b) Raman spectra of the pristine and annealed sample deposited on CG substrate.

Finally, *poly*-SiGe thin films were grown on Corning glass (CG) substrates to demonstrate the compatibility of this method for low thermal budget applications. The sample with the layer architecture *a*-$Si_{0.2}Ge_{0.8}$(100 nm)/AlO_x(~ 1nm)/*c*-Al(50 nm)/CG was annealed at 350 °C for 48 hours in N_2 ambient. The *poly*-SiGe phase that results upon the AIC annealing can be directly visualized in the optical micrograph (acquired from the backside of the CG substrate) shown in Figure 6(a). The *poly*-SiGe grains have an average size (diameter) of ~ 50 µm. The Raman spectra of the pristine and annealed sample (deposited on CG substrate) is shown in Figure 6(b). The Raman spectra of the pristine as well as the grain free region of the annealed sample show only amorphous features and contain no crystalline phases. Whereas the Raman spectrum acquired from within the grain of the annealed sample exhibit peaks at ~ 292 cm^{-1}, 398 cm^{-1} and 459 cm^{-1} corresponding to vibrational mode of Ge─Ge, Si─Ge and Si─Si bonds, respectively in the *poly*-SiGe phase. In this sample with the modified layer structure consisting of *a*-$Si_{0.2}Ge_{0.8}$, the thermal energy required for alloying is minimized and the supplied energy is mainly used in reorganizing grain boundaries thereby forming large grains. Thus, large grain *poly*-SiGe could be realized at 350 °C i.e. temperature lower than eutectic temperature of SiGe with Al as well as lower than glass softening temperature.

IV. CONCLUSION

In conclusion, *poly*-SiGe thin film could be achieved at low temperatures below 300 °C on Si substrate using catalytic Al induced crystallization. The alloying was found to be effective only in regions where Al induces a layer exchange in the crystallization process. In addition, the formation of *poly*-SiGe phase were found to be preceded by the formation of *a*-SiGe phase and depend on the isothermal annealing duration as well. Using the same mechanism, large grained *poly*-SiGe was also realized on corning glass at 350 °C. In this case, the *poly*-SiGe formation is not restricted to any particular region but there is an overall surface coverage. In both cases, *poly*-SiGe was achieved at temperature well below the eutectic temperature of Al-Ge and Al-Si system.

ACKNOWLEDGMENTS

The authors would like to thank the entire management of Sathyabama Institute of Science and Technology (Deemed to be University) for their support. The authors are highly grateful to Dr. Ch Kishan Singh from IGCAR, Kalpakkam for his immense help in carrying out the experiments, preparing and reviewing the manuscript. The authors would like to acknowledge Dr. S. R. Polaki, Dr. R.M. Sarguna and Dr. K. K. Madapu from IGCAR for their help during the experiments. The authors would also like to thank Directors, MSG and IGCAR for their support in this work.

| e-ISSN: 2319-8753, p-ISSN: 2347-6710| www.ijirset.com | Impact Factor: 8.423| A Monthly Peer Reviewed & Referred Journal |

|| Volume 13, Issue 4, April 2024 ||

| DOI:10.15680/IJIRSET.2024.1304086 |

REFERENCES

[1] C G Littlejohns et al Sci. Rep 5 8288 (2015)
[2] P Chaisakul et al Nat. Photonics 8 482 (2014)
[3] P Ashburn SiGe heterojunction bipolar transistors (John Wiley & Sons Ltd, UK) ISBN: 0-470- 84838-3 1 (2003)
[4] P M Mooney and J O Chu Annu. Rev. Mater. Sci 30 335 (2000)
[5] M Kurosawa, T Sadoh and M Miyao Thin Solid Films 518 S174 (2010)
[6] R Numata, K Toko, N Usami and T Suemasu Thin Solid Films 557 147 (2014)
[7] T Tah et al Mater. Sci Semicond. Process. 80 31 (2018)
[8] C K Singh et al J Non Cryst Solids 460 130 (2017)
[9] R Yoshimine, K Toko, and T Suemasu Jpn J Appl Phys 56 1 (2017)
[10] I Kabacelik, M Kulakci, and R Turan J Cryst Growth 419 7 (2015)
[11] S Y Yoon, S J Park, K H Kim and J Jang Thin Solid Films 383 34 (2001)
[12] S Peng, X Shen, Z Tang, and D He Mater Chem Phys 107 431 (2008)
[13] A Hamdoh, T Kaneko, and M Isomura Thin Solid Films 645 203 (2018)
[14] C Eisele et al Thin Solid Films 427 176 (2003)
[15] J Y Lin and P Y Chang Int. J. of Electr.Eng. 17 367 (2010)
[16] J Y Lin and P Y Chang Thin Solid Films 520 6893 (2012)
[17] F C Campbell Phase Diagrams - Understanding the basics (ASM International USA) 73 (2012)
[18] R Lechner, M Buschbeck, M Gjukic and M Stutzmann Phys. Status Solidi (C) 1 1131 (2004)
[19] Z Wang, L P H Jeurgens and E J Mittemeijer Metal Induced Crystallization (Taylor and Francis US) 25 (2015)
[20] C K Singh et al AIP Conf Proc 1731 080057 (2016)
[21] O Nast and A J Hartmann J. Appl. Phys 88 716 (2000)
[22] O Nast and S R Wenham J. Appl. Phys 88 124 (2000)
[23] K Gudrun and P Sergio Silicon, Germanium and Their Alloys (Taylor and Francis US) 23 (2015)

INTERNATIONAL STANDARD SERIAL NUMBER INDIA

INNO SPACE SJIF Scientific Journal Impact Factor

doi cross ref

निस्केयर NISCAIR

INTERNATIONAL JOURNAL OF INNOVATIVE RESEARCH

IN SCIENCE | ENGINEERING | TECHNOLOGY

9940 572 462 6381 907 438 ijirset@gmail.com

www.ijirset.com

Scan to save the contact details